

Dissecting the Cholera Toxin–Ganglioside GM1 Interaction by Isothermal Titration Calorimetry

W. Bruce Turnbull,[†] Bernie L. Precious,[‡] and Steve W. Homans^{*†}

Contribution from the Astbury Centre for Structural Molecular Biology, School of Biochemistry and Molecular Biology, University of Leeds, Leeds LS2 9JT, U.K., and Centre for Biomolecular Sciences, University of St. Andrews, St. Andrews KY16 9ST, U.K.

Received August 8, 2003; E-mail: s.w.homans@leeds.ac.uk

Abstract: The complex of cholera toxin and ganglioside GM1 is one of the highest affinity protein–carbohydrate interactions known. Herein, the GM1 pentasaccharide is dissected into smaller fragments to determine the contribution of each of the key monosaccharide residues to the overall binding affinity. Displacement isothermal titration calorimetry (ITC) has allowed the measurement of all of the key thermodynamic parameters for even the lowest affinity fragment ligands. Analysis of the standard free energy changes using Jencks' concept of intrinsic free energies reveals that the terminal galactose and sialic acid residues contribute 54% and 44% of the intrinsic binding energy, respectively, despite the latter ligand having little appreciable affinity for the toxin. This analysis also provides an estimate of 25.8 kJ mol⁻¹ for the loss of independent translational and rotational degrees of freedom on complexation and presents evidence for an alternative binding mode for ganglioside GM2. The high affinity and selectivity of the GM1–cholera toxin interaction originates principally from the conformational preorganization of the branched pentasaccharide rather than through the effect of cooperativity, which is also reinvestigated by ITC.

Introduction

Cell surface protein–carbohydrate interactions mediate the invasion and colonization of a wide range of pathogenic bacteria and viruses.¹ Furthermore, a number of bacteria, including *Clostridium tetani*, *Escherichia coli*, and *Vibrio cholerae*, also release protein toxins that similarly exploit adhesion to cell surface carbohydrates as a means of entering target cells,² usually of the gut wall. Such toxins are the primary virulence factors of many bacteria and the causative agents of tetanus, cholera, and haemolytic uremic syndrome among other diseases. The archetypal bacterial toxins are the cholera and heat-labile toxins derived from *V. cholerae* and *E. coli*, respectively. These toxins share an AB₅-type structure—a single A-subunit of 27 kDa which possesses a toxic ADP-ribosyltransferase activity and five identical B-subunits which bind selectively to the cell surface glycolipid ganglioside GM1 (Figure 1).³ The cholera toxin B-subunit (CTB)⁴ and heat-labile toxin B-subunit (LTB) share 80% sequence identity. CTB interacts with the soluble, monovalent oligosaccharide portion of GM1 (GM1os, **1**) with a micromolar dissociation constant at 37 °C,⁵ which places it among the highest affinity protein–carbohydrate interactions known. This binding is further enhanced through two mecha-

nisms: (1) through positive cooperativity between the protein subunits^{5–7} and (2) through the multivalent interaction of the pentameric toxin with up to five copies of GM1 at a cell surface;⁸ the micromolar affinity is thus amplified to give a nanomolar avidity.⁹ As CTB/LTB–GM1 adhesion is a prerequisite for the cell entry and thus subsequent activation of the toxin, there is a continuing interest in the design of high-affinity monovalent^{10–12} and multivalent¹³ inhibitors based on the oligosaccharide structure. Furthermore, as a consequence of its high affinity, the CTB–GM1os complex is an ideal system for

- (4) Gangliosides GM1, GM2, GM3, GA1, GD1b, and FucGM1 are abbreviated in the style of L. Svennerholm (*J. Neurochem.* **1963**, *10*, 613–623) and are illustrated in Figure 1. Other abbreviations: AFM, atomic force microscopy; CTB, cholera toxin B-subunit; Gal, galactose; GalNAc, *N*-acetylgalactosamine; GM1os, GM1 oligosaccharide; ITC, isothermal titration calorimetry; LTB, heat-labile toxin B-subunit; Neu5Ac, *N*-acetylneuraminic acid; SAR-by-NMR, structure–activity relationships by NMR spectroscopy; SPR, surface plasmon resonance; TLC, thin-layer chromatography.
- (5) Schön, A.; Freire, E. *Biochemistry* **1989**, *28*, 5019–5024.
- (6) (a) Sattler, J.; Schwarzmann, G.; Staerk, J.; Ziegler, W.; Wiegandt, H. *Hoppe-Seyler's Z. Physiol. Chem.* **1977**, *358*, 159–163. (b) Sattler, J.; Schwarzmann, G.; Knack, I.; Roehm, K. H.; Wiegandt, H. *Hoppe-Seyler's Z. Physiol. Chem.* **1978**, *359*, 719–723.
- (7) Schafer, D. E.; Thakur, A. K. *Cell Biophys.* **1982**, *4*, 25–40.
- (8) Mammen, M.; Choi, S. K.; Whitesides, G. M. *Angew. Chem., Int. Ed.* **1998**, *37*, 2755–2794.
- (9) Lauer, S.; Goldstein, B.; Nolan, R. L.; Nolan, J. P. *Biochemistry* **2002**, *41*, 1742–1751.
- (10) (a) Bernardi, A.; Checchia, A.; Brocca, P.; Sonnino, S.; Zuccotto, F. *J. Am. Chem. Soc.* **1999**, *121*, 2032–2036. (b) Minke, W. E.; Hong, F.; Verlinde, C. L. M. J.; Hol, W. G. J.; Fan, E. *J. Biol. Chem.* **1999**, *274*, 33469–33473. (c) Bernardi, A.; Arosio, D.; Sonnino, S. *Neurochem. Res.* **2002**, *27*, 539–545.
- (11) Pickens, J. C.; Merritt, E. A.; Ahn, M.; Verlinde, C. L. M. J.; Hol, W. G. J.; Fan, E. *Chem. Biol.* **2002**, *9*, 215–224.
- (12) Bernardi, A.; Arosio, D.; Manzoni, L.; Monti, D.; Posterl, H.; Potenza, D.; Mari, S.; Jimenez-Barbero, J. *Org. Biomol. Chem.* **2003**, *1*, 785–792.

[†] University of Leeds.

[‡] University of St. Andrews.

- (1) (a) Karlsson, K. A. *Annu. Rev. Biochem.* **1989**, *58*, 309–350. (b) Karlsson, K. A. *Mol. Microbiol.* **1998**, *29*, 1–11. (c) Menozzi, F. D.; Pethe, K.; Bifani, P.; Soncin, F.; Brennan, M. J.; Loch, C. *Mol. Microbiol.* **2002**, *43*, 1379–1386.
- (2) Merritt, E. A.; Hol, W. G. *J. Curr. Opin. Struct. Biol.* **1995**, *5*, 165–171.
- (3) Fukuta, S.; Magnani, J. L.; Twiddy, E. M.; Holmes, R. K.; Ginsburg, V. *Infect. Immun.* **1988**, *56*, 1748–1753.

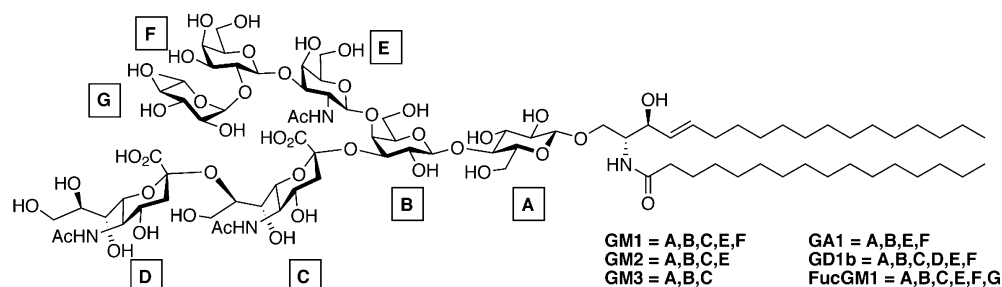


Figure 1. Composite structure of gangliosides used in binding studies with CTB.

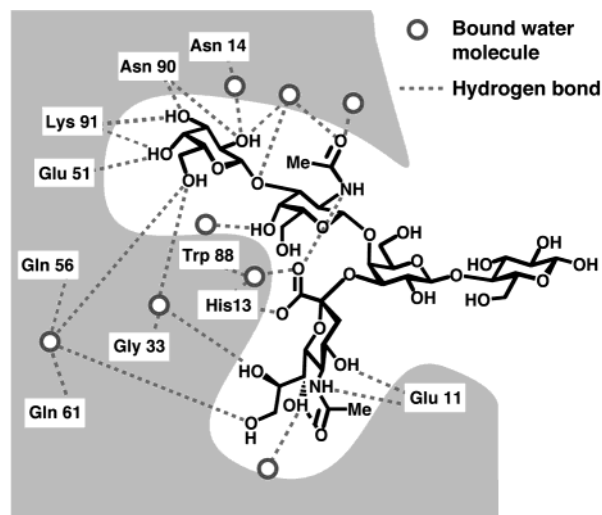


Figure 2. Schematic representation of the CTB–GM1os complex after Merritt et al., ref 14.

gaining further insight into the factors governing affinity and selectivity in protein–carbohydrate interactions.

The crystal structure of the CTB–GM1os complex has been refined to 1.25 Å resolution.^{14,15} It shows a bivalent interaction of the branched GM1os pentasaccharide, which has been likened to the carbohydrate holding the protein in a “two-fingered grip” comprising a sialic acid thumb and a Galβ(1→3)GalNAc forefinger (Figure 2). There are extensive intermolecular hydrogen-bonding contacts, both directly between the ligand and receptor and also via bridging water molecules. In terms of buried surface area, the terminal Gal, GalNAc, and Neu5Ac residues contribute 39%, 17%, and 43% of the intermolecular contacts.¹⁴ A large number of crystal structures of complexes between galactose derivatives and CTB or LTB have also been reported,^{11,16} including that of the Tn antigen,¹⁷ which represents the Galβ(1→3)GalNAc forefinger of GM1os. In all such complexes, the orientation of galactose and the structure of the binding site are essentially identical. Comparison of the

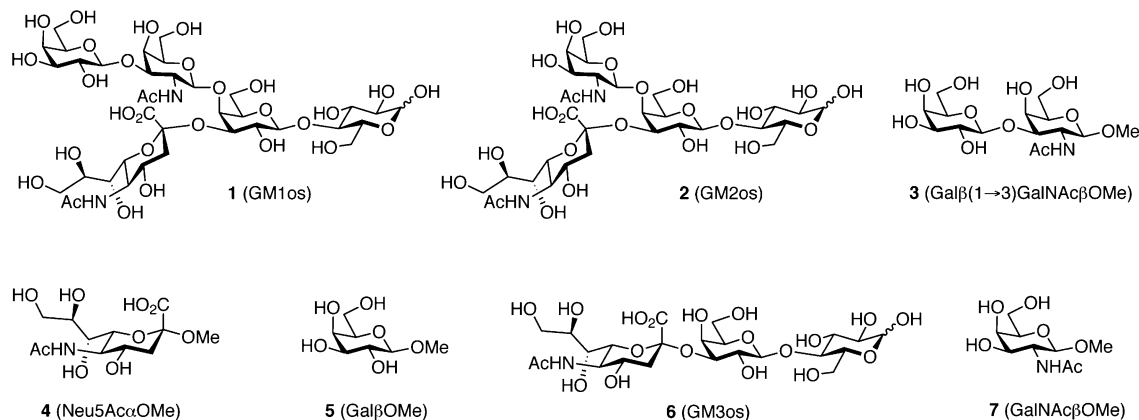
structures of the bound and free proteins reveals that there is only a small change to the backbone conformation (albeit mostly around the galactose binding site) on complexation.¹⁸ Furthermore, solution structures of GM1os indicate¹⁹ that the ligand is essentially preorganized for a near lock-and-key interaction with CTB.

Considering the importance of this interaction to the progression of cholera (and traveler’s diarrhea in the case of the *E. coli* heat-labile toxin), it is not surprising that there have been several studies reported on the selectivity and structural basis of complexation for GM1 and analogous ligands. Techniques as broad ranging as solid-phase and TLC overlay assays,^{3,20} surface plasmon resonance (SPR) biosensing,^{21,22} fluorescence spectroscopy^{23,24} and flow cytometry (FACS),⁹ atomic force microscopy (AFM),²⁵ and isothermal titration calorimetry (ITC)²⁶ have been applied to the problems of deconvoluting the kinetics and thermodynamics of this multivalent interaction and to rationalize the exquisite binding selectivity for GM1. The general trend in binding affinities/avidities that emerges from these studies is GM1 ≈ FucGM1 > GD1b ≫ GM2 > GA1 > GM3 (Figure 1).^{3,20,22,26,27} Structure–activity relationship studies of the sialic acid functional groups indicate that loss of the negative charge has a greater influence on affinity than removal/alteration of the acetamide group or glycerol side chain.²⁸

However, it is more difficult to extract precise information on the intrinsic contribution of each monosaccharide residue in the GM1 ligand from experiments conducted under multivalent conditions, as the mode of presentation of the ligand groups can strongly affect experimental results,²⁹ even giving quite conflicting views of intrinsic selectivities.^{21,22} Therefore, to try

- (13) (a) Thompson, J. P.; Schengrund, C.-L. *Biochem. Pharm.* **1998**, *56*, 591–597. (b) Vrasidas, I.; de Mol, N. J.; Liskamp, R. M. J.; Pieters, R. J. *Eur. J. Org. Chem.* **2001**, 4685–4692. (c) Merritt, E. A.; Zhang, Z.; Pickens, J. C.; Ahn, M.; Hol, W. G. J.; Fan, E. *J. Am. Chem. Soc.* **2002**, *124*, 8818–8824. (d) Zhang, Z.; Merritt, E. A.; Ahn, M.; Roach, C.; Hou, Z.; Verlinde, C. L. M. J.; Hol, W. G. J.; Fan, E. *J. Am. Chem. Soc.* **2002**, *124*, 12991–12998. (e) Schengrund, C. L. *Biochem. Pharm.* **2003**, *65*, 699–707.
- (14) Merritt, E. A.; Sarfaty, S.; van den Akker, F.; L’Hoir, C. L.; Martial, J. A.; Hol, W. G. *J. Protein Sci.* **1994**, *3*, 166–175.
- (15) Merritt, E. A.; Kuhn, P.; Sarfaty, S.; Erbe, J. L.; Holmes, R. K.; Hol, W. G. *J. Mol. Biol.* **1998**, *282*, 1043–1059.
- (16) (a) Merritt, E. A.; Sarfaty, S.; Feil, I. K.; Hol, W. G. *J. Structure* **1997**, *5*, 1485–1499. (b) Fan, E.; Merritt, E. A.; Zhang, Z.; Pickens, J. C.; Roach, C.; Ahn, M.; Hol, W. G. *J. Acta Crystallogr., D* **2001**, *D57*, 201–212.
- (17) van den Akker, F.; Steensma, E.; Hol, W. G. *J. Protein Sci.* **1996**, *5*, 1184–1188.

- (18) (a) Merritt, E. A.; Sixma, T. K.; Kalk, K. H.; van Zanten, B. A. M.; Hol, W. G. *J. Mol. Microbiol.* **1994**, *13*, 745–753. (b) Zhang, R. G.; Westbrook, M. L.; Westbrook, E. M.; Scott, D. L.; Otwinowski, Z.; Maulik, P. R.; Reed, R. A.; Shipley, G. G. *J. Mol. Biol.* **1995**, *251*, 550–562.
- (19) (a) Acquotti, D.; Poppe, L.; Dabrowski, J.; Vonderlieth, C. W.; Sonnino, S.; Tettamanti, G. *J. Am. Chem. Soc.* **1990**, *112*, 7772–7778. (b) Richardson, J. M.; Milton, M. J.; Homans, S. W. *J. Mol. Recog.* **1995**, *8*, 358–362. (c) Brocca, P.; Berthault, P.; Sonnino, S. *Biophys. J.* **1998**, *74*, 309–318. (d) Brocca, P.; Bernardi, A.; Raimondi, L.; Sonnino, S. *Glycoconjugate J.* **2001**, *17*, 283–299.
- (20) Ångström, J.; Teneberg, S.; Karlsson, K.-A. *Proc. Natl. Acad. Sci. U.S.A.* **1994**, *91*, 11859–11863.
- (21) Kuziemiako, G. M.; Stroh, M.; Stevens, R. C. *Biochemistry* **1996**, *35*, 6375–6384.
- (22) MacKenzie, C. R.; Hiramata, T.; Lee, K. K.; Altman, E.; Young, N. M. *J. Biol. Chem.* **1997**, *272*, 5533–5538.
- (23) Picking, W. L.; Moon, H.; Wu, H.; Picking, W. D. *Biochim. Biophys. Acta* **1995**, *1247*, 65–73.
- (24) Mertz, J. A.; McCann, J. A.; Picking, W. D. *Biochem. Biophys. Res. Commun.* **1996**, *226*, 140–144.
- (25) Cai, X.-E.; Yang, J. *Biochemistry* **2003**, *42*, 4028–4034.
- (26) Masserini, M.; Freire, E.; Palestini, P.; Calappi, E.; Tettamanti, G. *Biochemistry* **1992**, *31*, 2422–2426.
- (27) Schengrund, C. L.; Ringler, N. J. *J. Biol. Chem.* **1989**, *264*, 13233–13237.
- (28) (a) Lanne, B.; Schierbeck, B.; Karlsson, K.-A. *J. Biochem. (Tokyo)* **1994**, *116*, 1269–1274. (b) Lanne, B.; Schierbeck, B.; Ångström, J. *J. Biochem. (Tokyo)* **1999**, *126*, 226–234.

Chart 1. Ligands Used in the ITC Titrations

to understand how this particular protein–carbohydrate interaction works so efficiently, we have dissected the soluble GM1os pentasaccharide (**1**) into smaller fragments (Chart 1) and evaluated their intrinsic binding affinities for CTB using ITC.

Materials and Methods

CTB (>95% purity by SDS–PAGE) was purchased from Sigma, and the *E. coli* LTB was prepared according to published methods.³⁰ α -Methyl sialoside (**4**) was obtained from Chess (Germany), methyl β -galactopyranoside (**5**) was from Aldrich, and 3'-sialyl lactose (**6**) was from Dextra (U.K.). Compound **7** was prepared according to literature methods.³¹ All other reagents were purchased from Aldrich and were used without further purification. Full synthetic details for compounds **1–3** are given in the Supporting Information.

Isothermal Titration Calorimetry. ITC experiments were undertaken using either an MCS or VP-ITC calorimeter from Microcal Inc., with cell volumes of 1.309 and 1.409 mL, respectively. Unless stated otherwise, all ITC titrations were conducted at 25 °C in 50 mM Tris·HCl buffer at pH 7.4 containing 200 mM NaCl, 3 mM EDTA, and 1 mM Na₂S₂O₃. LTB-subunit concentrations of 145–265 μ M were used for direct titrations of GM1os fragments, and 10 μ M CTB-subunit was used for both direct and displacement titrations with GM1os. The protein was typically dialyzed twice against 2 L of Tris·HCl buffer. Ligand concentrations were determined by ¹H NMR spectroscopy against a 5 mM ethanol internal standard using a single-pulse experiment. Samples were then freeze-dried and redissolved in an appropriate volume of the same Tris·HCl buffer that had been used for protein dialysis. For displacement assays, CTB was preincubated with a high concentration (2–200 mM) of the low-affinity ligand and 110 μ M GM1os was titrated into the mixture. Typically, one 2 μ L injection and 25 μ L injections of ligand were added at 4 min intervals. The first data point was routinely deleted before curve fitting to allow for diffusion of ligand across the syringe tip during the pretitration equilibration period.

Nonlinear least-squares curve fitting was conducted in Microcal Origin using Microcal's one-site model, Sigurskjold's displacement model,³² or a multiple-interacting-sites model based on those described by Schafer and Thakur⁷ and Schön and Freire,⁵ but implemented using Microcal Origin LabTalk as described previously.³³ Heats of dilution were subtracted before curve fitting with the one-site and multiple-interacting-sites models, but in the case of the displacement model,

heat of dilution was accounted for during the fitting process according to Sigurskjold. No significant difference in the thermodynamic parameters was observed whether heat of dilution was used as a fitting parameter or measured in a blank titration of ligand into buffer. However, when using very high concentrations of the low-affinity ligand, e.g., for ligand **7**, it was preferable to add the same concentration of ligand to both the syringe and the cell to minimize dilution effects and modify Sigurskjold's fitting model accordingly.

Fluorescence Spectroscopy. Fluorescence titrations were conducted using a Perkin-Elmer LS50B luminescence spectrometer at 25 °C using an excitation wavelength of 290 nm and monitoring emission between 310 and 450 nm at a scan speed of 50 nm/min. Solutions of ligand **7** (0–500 mM) and CTB (1 μ M) were allowed to equilibrate for a few minutes prior to recording each spectrum. Data were analyzed in Origin 5.0 using the built-in binding model.

Results

Ligand Synthesis. To avoid any uncertainties associated with using anomeric mixtures of the smaller oligosaccharide fragments, the analogous methyl glycosides of Gal β (1→3)GalNAc (**3**), sialic acid (**4**), and galactose (**5**) were used for the ITC experiments. Disaccharide **3** was synthesized as described in the Supporting Information using an approach based on a literature synthesis of the analogous allyl glycoside.³⁴ In the case of **1** and its agalacto analogue GM2os (**2**), it was more convenient to synthesize the ligands by selective enzymatic degradation of bovine brain gangliosides.³⁵ Although the resulting oligosaccharides were obtained as anomeric mixtures, the CTB–GM1os crystal structure clearly indicates that the reducing terminal glucose residue points away from the protein and into solution and should therefore not have any effect on the binding thermodynamics.

ITC. In preliminary titration experiments using mono- to trisaccharide fragments of GM1os and LTB, all exhibited greater than millimolar K_d values. In the case of methyl galactoside **5**, this gave a hyperbolic curve even at relatively high protein concentration (145 μ M) (Figure 3a), but in the case of sialyl lactose **6**, no heat release beyond the heat of dilution was detected (Figure 3b). Although this observation could result from

(29) Horan, N.; Yan, L.; Isobe, H.; Whitesides, G. M.; Kahne, D. *Proc. Natl. Acad. Sci. U.S.A.* **1999**, *96*, 11782–11786.

(30) O'Dowd, A. M.; Botting, C. H.; Precious, B.; Shawcross, R.; Randall, R. E. *Vaccine* **1999**, *17*, 1442–1453.

(31) Tarasiejska, Z.; Jeanloz, R. W. *J. Am. Chem. Soc.* **1958**, *80*, 6325–6327. (a) Jacquinet, J. C.; Zurabyan, S. E.; Khorlin, A. Y. *Carbohydr. Res.* **1974**, *32*, 137–143.

(32) Sigurskjold, B. W. *Anal. Biochem.* **2000**, *277*, 260–266.

(33) Yung, A.; Turnbull, W. B.; Kalverda, A. P.; Thompson, G. S.; Homans, S. W.; Kitov, P.; Bundle, D. R. *J. Am. Chem. Soc.* **2003**, *125*, 13058–13062.

(34) (a) Lay, L.; Nicotra, F.; Panza, L.; Russo, G.; Adobati, E. *Helv. Chim. Acta* **1994**, *77*, 509–514. (b) Bernardi, A.; Boschin, G.; Checchia, A.; Lattanzio, M.; Manzoni, L.; Potenza, D.; Scolastico, C. *Eur. J. Org. Chem.* **1999**, 1311–1317.

(35) (a) Kolodny, E. H.; Brady, R. O.; Quirk, J. M.; Kanfer, J. N. *J. Lipid Res.* **1970**, *11*, 144–149. (b) Irie, R. F.; Tai, T.; Morton, D. L.; Cahan, L. D.; Paulson, J. C. U.S. Patent 4,557,931. (c) Ito, M. *Trends Glycosci. Glycotechnol.* **1990**, *2*, 399–402.

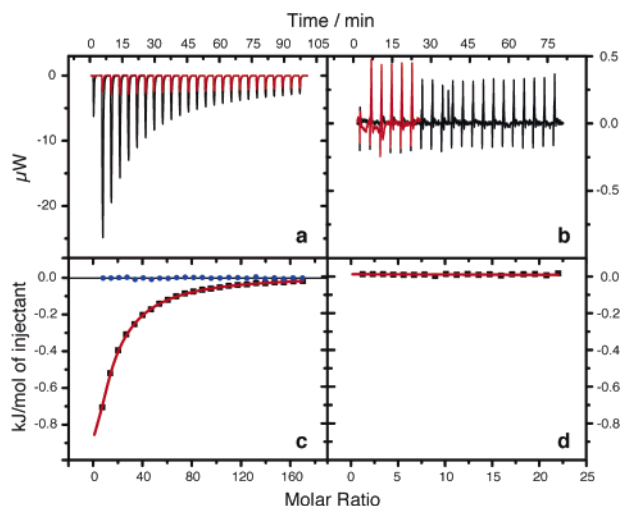


Figure 3. Titrations of LTB with (a) **5** and (b) sialyl lactose **6** with ligand dilution experiments conducted in the absence of protein overlaid in red. The corresponding integrated data are shown in panels c and d, respectively. Residuals of the curve fitting for the Gal β OMe data scaled up by a factor of 2 (panel c, blue circles) demonstrate the efficiency of the baseline subtraction of dilution processes.

either a very low ΔH° or a very low affinity, the difficulty in detecting binding of GM3 (Figure 1) to either LTB or CTB in multivalent binding assays^{9,20} would support the latter reason. Similarly, no interaction could be detected when sialyl lactose was added to a mixture of LTB and disaccharide **3**. Thus, the possibility of an intrasubunit cooperative effect in which the sialic acid binding affinity could be enhanced by the presence of a galactosyl ligand (acting to preorganize bridging water molecules in the binding site) was discounted.

Protein concentrations that are at least 10 times higher than the K_d are required to achieve titration curves with the sigmoidal shape that is preferred for curve fitting.³⁶ However, for weak interactions, such concentrations are often prohibitively high on account of protein solubility and/or availability. Although titrations employing protein concentrations below the K_d can still give reasonable estimates of the binding parameters,³⁷ an alternative approach that proved to be much more sensitive and economical in terms of protein consumption, while providing sigmoidal curves, was to use a displacement assay.³⁸ In this approach, a low concentration of the receptor is preincubated with the low-affinity ligand and then the high-affinity ligand is titrated into the mixture. A concise displacement model has been described³² previously for determining binding constants in systems with higher affinities than can be measured by conventional direct titration, as long as a lower affinity ligand with known thermodynamic parameters is available. The same model is also equally applicable for dealing with low-affinity interactions where a well-characterized higher affinity ligand is available.³⁹ However, this analysis assumes that each of the two competing ligands binds to the receptor following a simple two-state model. Whereas the effects of multivalency can be excluded from the experiments by using soluble monovalent GM1os, any cooperative effects will remain.

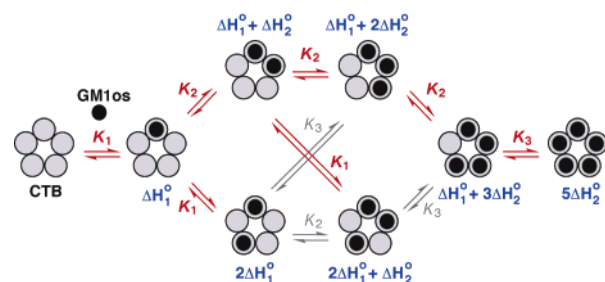


Figure 4. The interaction of CTB and GM1os can be described by a sequential binding model with 10 stepwise stability constants, 7 of which (shown in red) are sufficient to describe a path among all 8 states. Enthalpy changes relative to the unbound state are shown in blue.

Cooperativity was first identified⁶ from nonlinear Scatchard plots of equilibrium dialysis data which were fitted to the Hill equation to give a cooperativity coefficient of 1.25. This value lies toward the lower limit for positive cooperativity in a pentameric system which can exhibit values in the range of one (for no cooperativity) to five. Reanalysis of these data by Schafer and Thakur,⁷ using a model comprising seven independent stepwise binding constants, suggested a 2-fold increase in affinity for a second or subsequent molecules of GM1os binding to a CTB₅ pentamer. Schön and Freire employed⁵ a similar model for analyzing ITC data for the interaction. However, here the model was further constrained by the assumption that cooperativity would manifest itself only through nearest neighbor interactions and could thus be described by a ΔG for an isolated CTB–GM1os interaction and an additional cooperative enhancement of Δg for each adjacent filled binding site. An alternative description of this model (Figure 4) employs three binding constants

$$K_1 = e^{-\Delta G/RT}$$

$$K_2 = e^{-(\Delta G + \Delta g)/RT}$$

$$K_3 = e^{-(\Delta G + 2\Delta g)/RT}$$

with corresponding enthalpy changes

$$\Delta H_1^\circ = \Delta H$$

$$\Delta H_2^\circ = \Delta H + \Delta h$$

$$\Delta H_3^\circ = \Delta H + 2\Delta h$$

However, the model can be simplified further to only two stepwise equilibrium constants and two stepwise enthalpy changes as $K_1 K_3 = K_2 K_2$ and $\Delta H_1^\circ + \Delta H_3^\circ = 2\Delta H_2^\circ$. A more detailed account of the fitting equations for this model has been described elsewhere.³³

Schön and Freire concluded⁵ that where a ligand binds adjacent to a site that is already filled, there is a 4-fold increase in binding affinity accompanied by a change in the enthalpy of interaction from -22 to -33 kcal mol⁻¹. Such a dramatic difference in the stepwise enthalpy change should give rise to a binding isotherm that deviates significantly from the sigmoidal shape that is typical of the noninteracting sites model.⁴⁰ However, we were unable to reproduce these previous observa-

(36) Wiseman, T.; Williston, S.; Brandts, J. F.; Lin, L. N. *Anal. Biochem.* **1989**, *179*, 131–137.

(37) Turnbull, W. B.; Daranas, A. H. *J. Am. Chem. Soc.* **2003**, *125*, 14859–14866.

(38) Zhang, Y. L.; Zhang, Z. Y. *Anal. Biochem.* **1998**, *261*, 139–148.

(39) Christensen, T.; Gooden, D. M.; Kung, J. E.; Toone, E. J. *J. Am. Chem. Soc.* **2003**, *125*, 7357–7366.

(40) Fisher, H. F.; Tally, J. *Biochemistry* **1997**, *36*, 10807–10810.

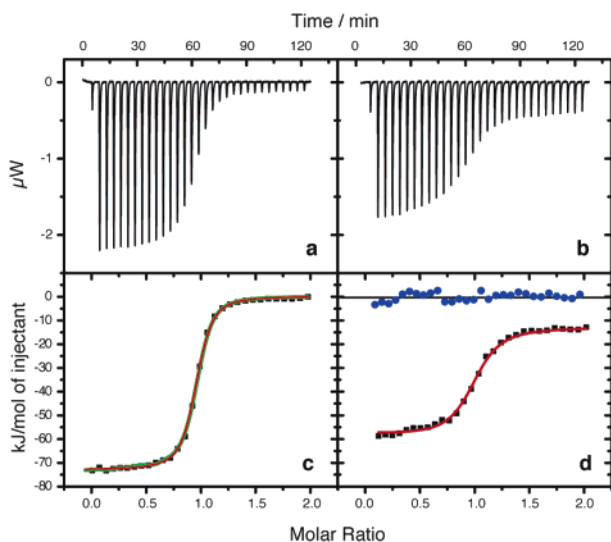


Figure 5. Titrations of 110 μM GM1os into 10 μM CTB in the absence (a) and presence (b) of 25 mM Gal β (1 \rightarrow 3)GalNAc β OMe. The best fitting curves based on the cooperative model (red) and noninteracting sites model (green) are shown in (c), and the displacement model (red) is shown in (d). Residuals of the curve fitting scaled up by a factor of 2 (blue circles in panel d) show that dilution processes have been accommodated adequately during analysis.

Table 1. Thermodynamic Parameters for GM1os Binding to CTB at 25 $^{\circ}\text{C}$ ^a

	cooperative model/ kJ mol^{-1}	noninteracting sites model/ kJ mol^{-1}		cooperative model/ kJ mol^{-1}	noninteracting sites model/ kJ mol^{-1}
ΔG_1°	-38.8 ± 0.1^b		$T\Delta S_1^{\circ}$	-35.0 ± 0.2	
ΔG_2°	-40.3 ± 0.1	-41.6 ± 0.1^c	$T\Delta S_2^{\circ}$	-32.2 ± 0.1	-30.8 ± 0.1
ΔH_1°	-73.8 ± 0.2				
ΔH_2°	-72.5 ± 0.1	-72.4 ± 0.1			

^a Binding stoichiometry was 1.004 ± 0.001 for the noninteracting sites model and is fixed at five ligands per CTB pentamer for the cooperative model. ^b Errors are those reported by Origin on the curve fitting. ^c The two models are equivalent if $\Delta G_1^{\circ} = \Delta G_2^{\circ}$, etc.

tions in any of our experiments, regardless of whether they were conducted at 15, 25, or 37 $^{\circ}\text{C}$, in either Tris \cdot HCl or phosphate buffer and using several different batches of CTB. In all cases, we found that the data fitted well to a simple noninteracting sites model, returning values for K and ΔH° that were independent of buffer ionization enthalpy. It was therefore decided to undertake a comparison of the standard one-site model and the cooperative model for the GM1os–CTB interaction.

As the binding constant at 25 $^{\circ}\text{C}$ is approaching the upper limit for direct titrations by ITC (on account of levels of signal-to-noise ratio),³⁶ data averaging was used to minimize random noise which can be better described by a model with more fitting parameters. Thus, data from three titrations, all run under identical conditions, were averaged and fitted using both the standard noninteracting sites model and the cooperative model (Figure 5a,c, Table 1). Although both models described the data well, an F -test⁴¹ demonstrated that the small improvement in fit for the cooperative model was nevertheless statistically significant (>95% probability) over and above the effect of having an extra variable fitting parameter compared to the one-site model. Therefore, our results are in accord with previous

observations of a cooperative effect giving a 2-fold increase in binding affinity.⁷

However, the values of ΔG_2° and ΔH_2° , which represent the average values for stepwise association constants and enthalpy changes when all five binding sites are filled, differ from ΔG° and ΔH° for the noninteracting sites model by only 3% and 0.2%, respectively. Furthermore, the apparent values of ΔG° and ΔH° resulting from the cooperative model vary by only 3.5% and 1.5%, respectively, during the course of the titration. Consequently, as cooperativity has not been observed for any fragments of GM1os,²⁴ the noninteracting sites approximation was adopted for curve fitting in displacement experiments. We would suggest that differences in our results from those reported by Schön and Freire may result from improvements in the sensitivity of calorimeters or in curve fitting associated with employing stepwise, rather than cumulative, enthalpy changes.³⁶

For the displacement titrations 10 μM CTB was pre-equilibrated with the low-affinity ligand prior to titration with GM1os. In all cases, sigmoidal curves demonstrating saturation of the receptor were still achieved on adding only 2 equiv of GM1os with respect to CTB-subunits. Figure 5b,d shows how the presence of 25 mM disaccharide **3** perturbs the GM1os–CTB titration curve. Compared to the curve for GM1os–CTB alone (Figure 5c), Gal β (1 \rightarrow 3)GalNAc β OMe reduces the apparent enthalpy of interaction and association constant for the curve, while increasing the heat of dilution that is apparent toward the end of the titration. This last phenomenon is a consequence of having a high concentration of the low-affinity ligand that is present in the cell, but absent from the injectant solution. In the case of **2**, initial curve fitting returned a binding stoichiometry of $n = 0.85$, whereas a second titration undertaken with identical samples of CTB and GM1os, but in the absence of **2**, gave $n = 1.00$. This observation would imply that 15% of the binding sites were already filled with the high-affinity ligand prior to starting the titration, which corresponds to 0.06% GM1os contaminating the sample of GM2os. Therefore, the total concentrations of GM1os at each step of the titration were recalculated using a modification of the equation used³⁷ in the Origin program:

$$[\text{X}]_{(i)} = \left([\text{X}]_0 + \frac{\Delta V_{(i)}[\text{X}]_{\text{syr}}}{V_0} \right) \left(1 - \frac{\Delta V_{(i)}}{2V_0} \right) \quad (1)$$

where $[\text{X}]_{(i)}$ is the GM1os concentration following the i th injection, $[\text{X}]_0$ is the initial concentration of GM1os in the cell prior to starting the titration, $\Delta V_{(i)}$ is the sum total volume of ligand added following the i th injection, $[\text{X}]_{\text{syr}}$ is the concentration of ligand in the syringe, and V_0 is the effective volume of the cell. The second bracketed term accounts for the fact that liquid is displaced from the sensitive part of the cell each time that an addition of ligand is made from the syringe. Curve fitting with these revised GM1os concentrations returned $n = 0.99$. Thermodynamic parameters obtained for all systems are listed in Table 2.

The dissociation constants vary over 7 orders of magnitude from the nanomolar range for the GM1os pentasaccharide **1** to the high millimolar range for methyl sialoside **4**. The errors returned by the fitting program are all small compared to the parameter values except for $T\Delta S^{\circ}$ for **2** (for which the parameter value is very low) and for methyl sialoside **4**. In the latter case,

(41) Gans, P. *Data fitting in the chemical sciences by the method of least squares*; Wiley: Chichester, U.K., 1992.

Table 2. Thermodynamic Parameters for GM1os and Its Fragment Ligands Binding to CTB at 25 °C

ligand	K_d /mM	ΔG° /kJ mol ⁻¹	ΔH° /kJ mol ⁻¹	$T\Delta S^\circ$ /kJ mol ⁻¹	n^b
1	$(4.33 \pm 0.14^a) \times 10^{-5}$	-41.6 ± 0.1	-72.4 ± 0.1	-30.8 ± 0.1	1.00
2	2.0 ± 0.2	-15.2 ± 0.2	-18.0 ± 2.0	-2.8 ± 2.0	0.99 ^c
3	7.6 ± 0.8	-12.0 ± 0.3	-42.1 ± 1.8	-30.1 ± 1.9	1.06
4	210 ± 100	-3.8 ± 1.2 $(-3.8 \pm 1.7)^d$	-44.4 ± 35.7	-40.6 ± 34.6	1.06
5	14.8 ± 1.6	-10.4 ± 0.3	-37.4 ± 2.0	-27.0 ± 2.0	0.94
7	118 ± 12	-5.3 ± 0.2	-38.4 ± 1.9	-33.1 ± 1.9	1.04

^a Errors are those reported by Origin on the curve fitting. ^b All errors on binding stoichiometries were reported to be less than 1%. ^c Adjusted value taking into account the presence of 1.5 μ M GM1os present in the GM2os/CTB mixture at the start of the titration. ^d Value and error used in subsequent calculations (see the text).

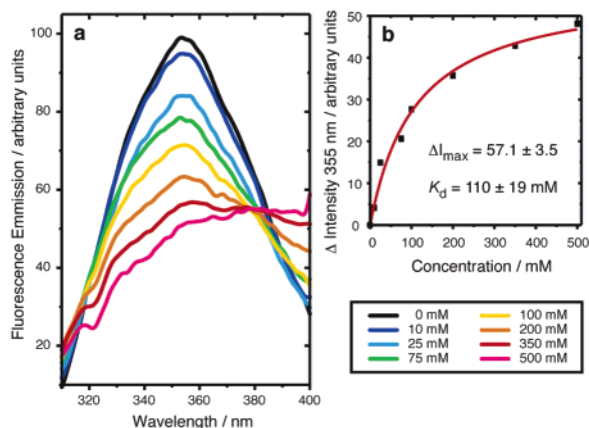


Figure 6. (a) Quenching of the CTB–Trp88 fluorescence with increasing concentrations of GalNAc β OME is described well by (b) a simple two-state binding model.

the errors originate from the broad minimum in the 3-D surface defining the curve fitting process. Extensive simulations revealed that reasonable combinations of K_d and ΔH° lay in a steep-walled valley running from $K_d = 100$ mM/ $\Delta H^\circ = -21$ kJ mol⁻¹ to $K_d = 400$ mM/ $\Delta H^\circ = -79$ kJ mol⁻¹. Consequently, a ΔG° value of -3.8 ± 1.7 kJ mol⁻¹ for methyl sialoside was carried through subsequent calculations. Duplicate displacement experiments returned values of K_d that were within $\pm 20\%$ of the values listed above and $\pm 7\%$ for direct titrations run in triplicate with GM1os. As these errors were larger than those for the precision of the fitting reported in Table 2, the corresponding errors in ΔG° of ± 0.5 kJ mol⁻¹ (for **2**, **3**, and **5**) and ± 0.2 kJ mol⁻¹ (for **1**) were used in subsequent calculations.

The interaction of GalNAc β OME (**7**) was studied by both displacement ITC and fluorescence titration (Figure 6). The sole tryptophan residue in CTB is located at the bottom of the galactose binding site where its indole ring stacks against the hydrophobic α -face of the galactosyl residue. It is well established that, on close interaction with this group, the fluorescence spectrum of CTB exhibits a change in intensity and/or a shift in its wavelength for maximum emission.^{12,24} The fact that both assays return identical dissociation constants (ca. 110 mM) further validates the displacement ITC method for measuring low-affinity interactions and also indicates that, in the absence of a galactose residue, GalNAc β OME will instead occupy the galactose binding site, albeit with a reduced affinity compared to Gal β OME (**5**).

Discussion

From the results in Table 2, it is clear that the sum of ΔG° for complementary fragments of GM1os (i.e., **2** + **5** and **3** +

4), falls a long way short of ΔG° for the bivalent ligand. This is perhaps not surprising, as Jencks has noted⁴² that ΔG° for fragments of a bivalent ligand should not be additive as a consequence of the entropic penalty to be paid on complex formation that results from a loss of independent rotational and translational degrees of freedom for the ligand and receptor. Whereas for a bivalent ligand this penalty is paid only once, in the case of two complementary fragments binding to the receptor to form a ternary complex, this penalty would be paid twice. Consequently, Jencks recommended invoking the concept of *intrinsic free energy change* ΔG^i , which is defined as the change in free energy on complexation in the absence of the entropic penalty described above. In other words, once half of a bivalent ligand has bound to its receptor, the ligand has already paid the entropic penalty for complex formation, so the second half of the ligand now interacts with an enhanced intrinsic affinity, $\Delta G^i = -RT \ln K^i$. Therefore, ΔG^i for a fragment of a ligand is a measure of the contribution that fragment makes to the overall interaction. For systems in which there is no significant change in the structure of either the ligand or the receptor on binding, ΔG^i for a fragment of a bivalent ligand can be estimated, to a first approximation, by determining the shortfall in ΔG° of the complementary fragment with respect to ΔG° for the full bivalent ligand:

$$\Delta G_A^i = \Delta G_{AB}^\circ - \Delta G_B^\circ \quad (2)$$

Thus, ΔG^i for the galactose residue can be estimated by subtracting ΔG° for GM2os from ΔG° for GM1os. Furthermore, whereas ΔG° values for fragment ligands are not additive, their intrinsic free energies are:

$$\Delta G_{AB}^i = \Delta G_A^i + \Delta G_B^i \quad (3)$$

Thus, ΔG^i for GM1os can be calculated by adding ΔG^i for both fragments **3** and **4**. Finally, the difference between ΔG° and ΔG^i for GM1os is a measure of the largely entropic penalty to be paid on bringing two particles together to form a complex. Jencks referred to this as the Gibbs connection energy (ΔG^s), and for an ideal system this parameter also accounts for the shortfall in the sum of ΔG° for the fragment ligands relative to ΔG° for the bivalent ligand:

$$\Delta G^s = \Delta G_{AB}^\circ - \Delta G_{AB}^i = (\Delta G_A^\circ + \Delta G_B^\circ) - \Delta G_{AB}^\circ \quad (4)$$

A summary of the standard, intrinsic, and connection free energy changes are given in Figure 7. An initial analysis of the data, however, provides inconsistent values for ΔG^s depending

(42) Jencks, W. P. *Proc. Natl. Acad. Sci. U.S.A.* **1981**, *78*, 4046–4050.

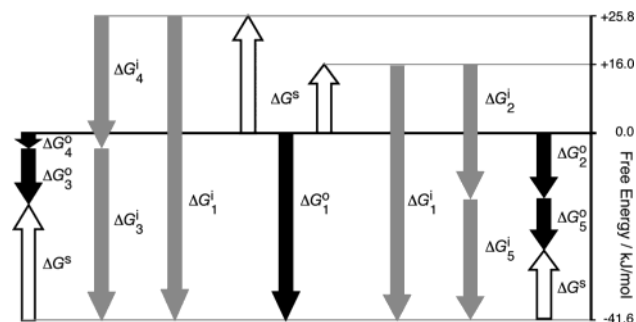


Figure 7. Summary of the free energy changes for ligands 1–5. Standard free energy changes are shown in black, intrinsic free energy changes in gray, and Gibbs connection energies in white. Up and down arrows indicate positive and negative changes, respectively.

on which disconnection (i.e., Gal β OME/GM2os or Neu5Ac α OME/Gal β (1 \rightarrow 3)GalNAcOME) is chosen for the calculation. The most likely explanation for this observation is that one (or more) of the ligands binds to the receptor in a position that is distinct from the site occupied by the corresponding fragment of GM1os. Such “nonproductive binding”⁴² will only occur if the fragment ligand finds a higher affinity site in the absence of its complementary fragment, or in other words, binding of a fragment to its preferred site is destabilized once part of the bivalent ligand. Considering that crystallographic data are available for complexes of a wide range of galactose derivatives, all of which show the galactose residue bound in an identical orientation, yet no structures have been published for either the GM2os or sialic acid complexes, it is most probable that it is one of these complexes that differs from that predicted using the GM1os–CTB structure. This hypothesis is reinforced by the observation that the 50–200-fold increase in the binding affinity of GM2os vs Neu5Ac α OME is far greater than can be accounted for by the intrinsic free energy change for the additional GalNAc residue of 1.4 kJ mol⁻¹ (calculated from $\Delta G_{\text{GalNAc}}^i = \Delta G_{\text{GalGalNAc}}^\circ - \Delta G_{\text{Gal}}^\circ$).

It follows from eq 3 that

$$\Delta G_A^\circ + \Delta G_B^\circ = \Delta G_{A'}^\circ + \Delta G_{B'}^\circ = \Delta G_{AB}^\circ + \Delta G^s \quad (5)$$

where A–B and A'–B' are pairs of complementary fragments resulting from different disconnections of bivalent ligand AB. Therefore, by knowing ΔG° for three of the fragment ligands, it is possible to estimate what ΔG° for the fourth ligand should be. Such a calculation would predict that the sialoside fragment **4** should have a K_d of 4 mM, which is considerably higher affinity than the observed value. Alternatively, if the K_d for Neu5Ac α OME is assumed to be 100–400 mM, then GM2os should have a K_d of ca. 50–200 mM ($\Delta G^\circ = -5.4 \pm 1.8$ kJ mol⁻¹, based on $\Delta G^\circ = -3.8 \pm 1.7$ kJ mol⁻¹ for **4**)—a much lower affinity than is measured experimentally. This would be feasible if the GM2os tetrasaccharide does not bind to CTB in the same orientation as the corresponding fragment of GM1os, but rather it finds a higher affinity site elsewhere on the receptor.

Similarly, on the basis of ΔG^i for GalNAc, it would be expected that **7** should have no measurable affinity for the protein. However, **7** does bind to CTB, albeit weakly, as is evident from both calorimetric and fluorimetric experiments. Moreover, in this case, the fluorescence titrations provide compelling evidence for a shift in binding site to that occupied by the terminal galactose residue in GM1os. Taking into

Table 3. Summary of Revised Intrinsic Free Energies for GM1os and Its Fragment Ligands Binding to CTB at 25 °C

fragment	ΔG^{aj} kJ mol ⁻¹	% $\Delta G_{\text{GM1os}}^i$	% BSA GM1os–CTB ^c
GM1os	-67.4 ± 1.9	100	100
GM2os	-31.2 ± 0.5	46	60
Gal β (1 \rightarrow 3)GalNAc	-37.8 ± 1.7	56	56
α -Neu5Ac	-29.6 ± 0.5	44	43
β -Gal	-36.2 ± 1.8	54	39
β -GalNAc	-1.6 ± 0.7^b	2	17

^a Revised values assuming $\Delta G^\circ = -5.4 \pm 1.8$ kJ mol⁻¹ for GM2os binding to CTB in the same orientation as GM1os. ^b Based on $\Delta G_{\text{GalNAc}}^i = \Delta G_{\text{GalGalNAc}}^\circ - \Delta G_{\text{Gal}}^\circ$. ^c Change in buried surface area for GM1os–CTB interaction as reported in ref 14.

consideration that GalNAc β OME binds in this site with a higher affinity than Neu5Ac α OME alone has for CTB, it is not unreasonable to predict that, in the absence of the terminal galactose residue, the GM2os fragment instead occupies the galactose binding site while repositioning the sialic acid residue to give alternative additional contacts with the protein. This hypothesis would account for the observation^{3,20,27} that, at a multivalent surface, CTB/LTB binds more strongly to GM2 than to GA1, yet shows no appreciable affinity for GM3. Furthermore, the ability of the galactose binding site to accommodate substitutions at C-2 of the ligand is consistent with the reported similar affinities of GM1 and fucosyl-GM1 (fucGM1) for the toxin.²⁶ Although, in theory, this hypothesis could be tested by fluorescence titration, the experiment was precluded in the current study by the fact that the GM2os was contaminated by ca. 0.06% GM1os. Although this contaminant was too low to be detected by HPLC, NMR spectroscopy, or electrospray mass spectrometry, a reduction in the binding stoichiometry was detected in the ITC experiment corresponding to partial occupancy of the CTB binding site prior to starting the displacement titration. Whereas the contaminating GM1os could be accommodated explicitly in calculating the thermodynamic parameters for this displacement titration, it would be impossible to distinguish the effect on CTB fluorescence of GM2os from that of the much higher affinity GM1os.

A revised breakdown of the intrinsic free energy contributions, employing the predicted value of ΔG° for GM2os, is given in Table 3. The Gibbs connection energy is calculated to be 25.8 ± 1.9 kJ mol⁻¹ at 298 K. There have been several estimates for ΔG^i published varying from 8.7 to over 80 kJ mol⁻¹ at 298 K.⁴³ Bearing in mind that no real system exhibits ideal behavior, the current analysis should give only lower limits to the values of ΔG^i and ΔG^s . It is therefore worth noting that following a review of the published literature, Lundquist and Toone concluded that “the interaction free energy is likely no greater than 6 kcal mol⁻¹” (ca. 25 kJ mol⁻¹).⁴⁴

Derivation of intrinsic free energy changes also allows a means of dissecting the individual contributions of each of the three key monosaccharide residues that participate in the interaction with CTB. The results summarized in Table 3 correlate reasonably well with a similar division of the change in buried surface area on binding that was previously calculated from the crystal structure of the complex. It is interesting to

(43) Burkhalter, N. F.; Dimick, S. M.; Toone, E. J. In *Carbohydrates in Chemistry and Biology. Part I: Chemistry of Saccharides*; Ernst, B., Hart, G. W., Pierre, S., Eds.; Wiley-VCH: Weinheim, Germany, 2000; Vol. 2, pp 863–914.

(44) Lundquist, J. J.; Toone, E. J. *Chem. Rev.* **2002**, *102*, 555–578.

note that the sialic acid residue contributes almost half of the stability of the complex even though, in isolation, this monosaccharide has little appreciable affinity for the receptor. Drug discovery strategies such as SAR-by-NMR⁴⁵ rely on identifying small molecules that may be accommodated simultaneously in a receptor binding site and subsequently tethered together to form high-affinity ligands. Considering the very poor 200 mM K_d for Neu5Ac α OMe, it is unlikely that the GM1os ligand would have been discovered by such an approach! Of course, in this case it is presumably the CTB receptor that has evolved to exploit ligands available in mammalian glycobiology, rather than vice versa.

Furthermore, the importance of linker design in such a strategy is highlighted by a GM1os analogue synthesized by Hindsgaul and co-workers in which the internal lactose unit is replaced by a simple ethylene linker between the sialic acid and GalNAc residues.⁴⁶ This GM1os analogue binds with a micromolar affinity corresponding to an unfavorable $\Delta\Delta G^\circ$ of ca. 8 kJ mol⁻¹ relative to GM1os. It is the relative rigidity of the GM1os pentasaccharide, which is preorganized in a conformation suitable for binding, that confers its impressive selectivity over related oligosaccharide ligands and allows a reasonable estimate of ΔG° to be made using this system. Indeed, synthetic linkers designed to mimic the rigid conformation of the internal galactosyl residue provide GM1 analogues with affinities for CTB similar to those for the natural ligand.^{10a,c,12} However, it must be expected that there will still be some loss of residual conformational entropy upon binding. Therefore, as this analysis has assumed that both ligand and receptor are rigid bodies, it is possible that both ΔG° and the contribution of the GalNAc residue have been underestimated. Nevertheless, it is unlikely that the contribution of the GalNAc residue would rise above 10% of the total, so its role in the complex is probably less supramolecular than structural, acting to hold the sialic acid and galactose residues in the appropriate spatial arrangement for complexation.

Analysis of the enthalpic and entropic contributions to the free energy changes goes further to support this conclusion. Addition of the GalNAc residue to the terminal galactose provides a modest increase in ΔH° which is largely offset by a similar increase in the unfavorable entropy term. However, from here, there is virtually no further change in the entropic term upon introducing the sialic acid residue into the ligand. The net contribution of the sialic acid is almost entirely enthalpic, enabling a favorable increase of -26.4 kJ mol⁻¹ in the free energy term. It is worth noting that the balance of enthalpic and entropic contributions giving rise to the more favorable

affinity for GM2os is very different from that of the ligands that bear a terminal galactose residue. However, in the absence of structural information for this complex, further discussion would be inappropriate.

Conclusions

The relatively high monovalent affinity of GM1 for CTB arises from the extensive intermolecular contacts between a ligand and receptor that are essentially preorganized for binding. On the other hand, the high selectivity of this interaction arises from having the two key monosaccharide recognition sites separated in the oligosaccharide by two other residues, thus preventing any corresponding fragments of GM1os from achieving interactions of comparable efficiency. That high-affinity ligands can be achieved through a chelation strategy is certainly not a new concept, but the extent to which gains in ΔG° can be achieved in cases for which the structure of the linker is optimal is less well appreciated. Ligands with poor affinities in the millimolar range are conventionally dismissed as inactive, yet here, Nature makes efficient use of weakly binding building blocks to construct ligands of great functional importance.

Jencks' concept of intrinsic free energy changes provides a useful framework for dissecting the contributions of individual fragments of a complicated ligand. Such an analysis has provided an estimate of 25.8 ± 1.9 kJ mol⁻¹ for the entropic penalty to be paid on bringing two molecules together to form a complex. Furthermore, this analysis has led us to consider that the selectivity of the toxin for GM2 over GA1 may be a consequence of GM2 binding in a manner that differs from that of the corresponding fragment of GM1—a hypothesis that remains to be tested. Determination of the intrinsic contributions of each monosaccharide residue to the overall interaction can also provide direction in the rational design of GM1os analogues. This work supports the strategy that has been followed^{11,12} to date in using galactose as a source of selectivity in ligand design, but it also emphasizes the potential gains that may be had from further exploring the conformational space occupied by the sialic acid residue in GM1os.

Acknowledgment. This work was supported through the award of a Wellcome Trust International Prize Travelling Research Fellowship to W.B.T. The VP-ITC unit was funded through a Joint Infrastructure Fund award. We thank Dr. B. W. Sigurskjold for providing definition files for his displacement model.

Supporting Information Available: Experimental details for the preparation of compounds 1–3. This material is available free of charge via the Internet at <http://pubs.acs.org>.

JA0378207

(45) Shuker, S. B.; Hajduk, P. J.; Meadows, R. P.; Fesik, S. W. *Science* **1996**, *274*, 1531–1534.

(46) Hindsgaul, O.; Schriemer, D. C. U.S. Patent 6,054,047, 2000.